Electron Localization or Delocalization in Incommensurate Helical Magnets

Shu Tanaka,[1,*] Hosho Katsura,[2] and Naoto Nagaosa[2,3,4]

[1]*Department of Physics, The University of Tokyo, 7-3-1, Hongo, Bunkyo-ku, Tokyo 113-0033, Japan*
[2]*Department of Applied Physics, The University of Tokyo, 7-3-1, Hongo, Bunkyo-ku, Tokyo 113-8656, Japan*
[3]*Correlated Electron Research Center (CERC), National Institute of Advanced Industrial Science and Technology (AIST), Tsukuba Central 4, Tsukuba 305-8562, Japan*
[4]*CREST, Japan Science and Technology Agency (JST), Saitama, 332-0012, Japan*

(Received 20 March 2006; published 15 September 2006)

The electronic states in incommensurate helical magnets are studied theoretically from the viewpoint of the localization or delocalization. It is found that in the multiband system with a relativistic spin-orbit interaction, the electronic wave functions show both an extended and localized nature along the helical axis depending on the orbital, helical wave number, and the direction of the plane on which spins rotate. The possible realization of this localization is discussed.

DOI: 10.1103/PhysRevLett.97.116404 PACS numbers: 71.23.An, 71.70.Ej, 75.30.−m

Helical magnets have been studied for a long time since their first discovery by Yoshimori [1]. Their ground states are determined by the (frustrated) exchange interactions and their Fourier transformation $J(q)$. Various properties including the spin wave excitations are analyzed theoretically for many materials (see [2] for an early review). Helical spin structure is recently attracting revived interest from the viewpoint of both dielectric and transport properties. One example is the ferroelectricity induced by the helical magnetic order. Theoretically, the spin current associated with the noncollinear spin configuration is proposed to induce the electric polarization [3]. Experimentally, it is now found that this mechanism is at work in $R\mathrm{MnO}_3$ [4–6] and in other materials [7–10]. Another new aspect is the anomalous transport properties associated with the onset of helical spin structure in metallic systems such as β-MnO_2 [11], SrFeO_3 [12,13], and MnSi, (Fe,Co)Si [14]. These developments urge the microscopic theory of electronic states to understand the physical properties associated with the helical spins.

In the absence of the spin-orbit interaction (SOI), one can rotate the spin frame so that the z axis is parallel to the direction of the local spin. In this rotated frame, the spins are aligned ferromagnetically and the original spin structure is reflected in the magnitude and phase of the effective transfer integrals. This leads to the double exchange interaction [15] and various phenomena related to the spin chirality [16,17], respectively. When we consider the state of single helical wave vector q, the relative angle between the neighboring spins does not break the original translational symmetry. Furthermore, there is no spin chirality, i.e., no fictitious magnetic field induced by the solid angle subtended by the spins. Therefore the Hamiltonian in the rotated spin frame preserves the periodicity of the original lattice, and hence one can define the Bloch wave function.

This situation is modified in an essential way when the SOI is taken into account. In this case, one cannot rotate the spin frame with the orbitals being intact, and the transfer integrals forming a matrix between ions are transformed in a nontrivial way. Therefore, in general, we expect the incommensurate (IC) modulation of the transfer integrals and even of the site energies in the effective Hamiltonian in the rotated frame.

The localization or delocalization (L-DL) of electronic states in an IC potential is an old issue [18]. Unlike in the case of commensurate periodic potentials, the eigenstates are not the extended Bloch states in the case of IC potentials. Therefore the band structures would be unusual, i.e., highly fragmented, in those IC potentials. The central issue is whether electronic states are extended or localized in this kind of potentials, namely, metal-insulator transition (MIT). Aubry and Andre (A-A) [19] have shown that in a simple 1D model MIT occurs simultaneously for all energies when the strength of the IC potential V_0 is equal to the transfer integral t; i.e., if V_0 is greater than t, the electronic states localize. We can also regard the A-A model as a two dimensional tight binding model with IC magnetic flux. Actually, the well-known Hofstadter butterfly is closely related to this model [20]. Using the *trace map* technique, Kohmoto *et al.* [21] has exactly studied the scaling properties of the Fibonacci lattice system, which can be regarded as the A-A model with IC modulation $Qa/2\pi$ being the inverse golden mean. Similar problems with the IC transfer integral are also investigated by Kohmoto *et al.* [22].

In this Letter we investigate the L-DL of electronic states in IC helical magnets. First, we study a model of $5d$ orbitals in cubic symmetry taking into account the SOI. We found that as SOI increases, the localization caused by IC starts from the specific t_{2g} wave functions at around $q \sim \pi/a$ (a: lattice constant). In order to scrutinize this localization, we construct an effective single-band model for t_{2g} bands. With this effective model, the localization lengths are studied in more detail including its dependence on the angle φ between the spin rotation angle and the helical wave vector.

We start with the following electronic model:

$$H = H_U + H_{\mathrm{SO}} + H_d + H_t,$$
$$H_U = -U\sum_j \vec{e}_j \cdot \vec{S}_j, \qquad H_{\mathrm{SO}} = -\lambda\sum_j \vec{L}_j \cdot \vec{S}_j, \tag{1}$$
$$H_d = \sum_j \epsilon_\alpha |d^\alpha_{j\sigma}\rangle\langle d^\alpha_{j\sigma}|, \qquad H_t = \sum_{\langle i,j\rangle} t^\alpha_{ij} |d^\alpha_{j\sigma}\rangle\langle d^\alpha_{i\sigma}|.$$

In the octahedral ligand field, the d orbitals are split into e_g and t_{2g} orbitals [23]. The t_{2g} orbitals, i.e., d^{xy}, d^{yz}, and d^{zx}, have energies lower than e_g orbitals, i.e., $d^{x^2-y^2}$, and $d^{3z^2-r^2}$ by $10Dq$, but the order is reversed as we take the hole picture in the following, i.e., $\epsilon_{t_{2g}} - \epsilon_{e_g} = 10Dq$. The on-site SOI is considered, the matrix elements of which are calculated by $\vec{L}\cdot\vec{S}$ with $\vec{L}$ ($\vec{S}$) being the orbital (spin) angular momentum. It is noted that $\vec{L}$ has no matrix elements within the e_g sector, while nonzero coupling occurs within the t_{2g} sector and between the e_g and t_{2g} sectors. Considering the hopping between d orbitals and oxygen orbitals [24], we derive the effective transfer integrals t^α_{ij} between d^α orbitals at neighboring magnetic ions i and j. We took the values $t^{yz} = t^{zx} = 0.1$, $t^{3z^2-r^2} = 0.3$, and $t^{xy} = t^{x^2-y^2} = 0$. In H_U of Eq. (1), the magnetic moment at site j is described by the unit vector $\vec{e}_j \equiv (\cos\phi_j \sin\theta_j, \sin\phi_j \sin\theta_j, \cos\theta_j)$ and $\vec{S}_j$ denotes the electronic spin operator at site j. We assume the IC helical magnetic structure for $\vec{S}_j$ along z axis, which is on the spin zx plane, realized as a result of the frustrated spin exchange interaction. We focus on the ordered ground state properties, and hence the mean field treatment gives a good description of the system. We assume the ferromagnetic spin configuration perpendicular to the helical wave vector $\vec{q}$, and hence k_x, k_y are good quantum numbers; i.e., the electronic wave functions are plane waves along x and y directions. We fix $k_x = k_y = 0$ hereafter, and consider the one-dimensional (1D) model only along the z direction. Figure 1 shows the calculated density of states as a function of the helical wave number q with the color specifying the localization length ξ. We note here that the sample size is a prime number 199, and helical wave numbers q's are taken to be proximate to the IC values. All the band states from the e_g orbitals are extended due to the weak SOI, and hence are omitted in Fig. 1. The green region is the extended states, while the blue one is strongly localized within the scale of lattice constant. We took the values $10Dq = 3$, $U = 1.4$, and $\lambda = 1.0$.

The density of states are understood as follows. The largest splitting between e_g and t_{2g} occurs due to the ligand field $10Dq$ in Eq. (1). Then the t_{2g} bands are further split into bands of Γ_7 and Γ_8 origin, the latter of which is upper in energy since we take the hole picture. Then both the bands are further split by the spin exchange field U.

By using the iterative method developed by MacKinnon [25], we can calculate the Green's function $G^{(N)}_{1,N} \equiv \langle 1|(E-H)^{-1}|N\rangle$, which connects both ends of the long chain. $G^{(N)}_{1,N}$ is still a 10×10 matrix and the Lyapnov exponent; i.e., the inverse of the localization length ξ is obtained as $\frac{1}{\xi} \equiv -\lim_{N\to\infty}\frac{1}{2N}\ln\mathrm{Tr}|G^{(N)}_{1,N}|^2$. The blue color at around $q \sim \pi/a$ means the strong localization along the helical axis. When we change λ, we still observe the localization down to $\lambda \sim 0.2$. Therefore, we conclude that the localization starts in some part of the electronic spectrum at around $q = \pi/a$ as one increases the SOI. The most remarkable point we can grasp from the above figure is that there are both localized and extended states at different energies for the same q [26]. This is in sharp contrast to the case of the A-A model where all the states are either extended or localized depending only on the ratio V_0/t as mentioned above.

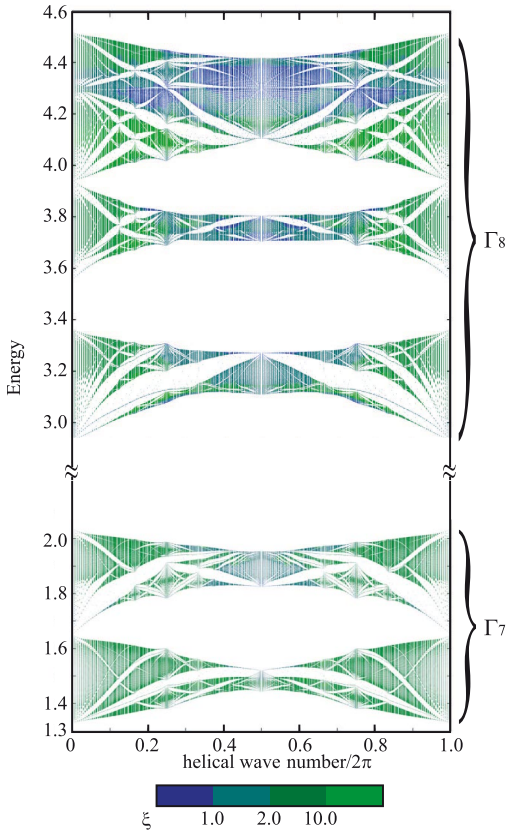

FIG. 1 (color online). Density of states and color map of the localization length ξ on it for the d-orbital model Eq. (1).

In order to study this localization in more depth, we now derive the effective model for a limiting case, i.e., $10Dq \gg 3\lambda/2 \gg U \gg t$. Even though this is not necessarily a suitable limit for realistic systems, it clarifies why ξ depends on the orbitals. By taking into account the spin degree of freedom, there is sixfold degeneracy of the t_{2g} energy levels. Because of the on-site SOI, this degeneracy is lifted and we have two groups of spin-orbit coupled states, labeled Γ_7 and Γ_8 [23]. The twofold degenerate states, Γ_7, and the fourfold degenerate one, Γ_8, are given

by $|3^+\rangle = (|d_\uparrow^{xy}\rangle + |d_\downarrow^{yz}\rangle + i|d_\downarrow^{zx}\rangle)/\sqrt{3}$, $|3^-\rangle = (|d_\downarrow^{xy}\rangle - |d_\uparrow^{yz}\rangle + i|d_\uparrow^{zx}\rangle)/\sqrt{3}$, and $|1^+\rangle = (|d_\uparrow^{yz}\rangle + i|d_\uparrow^{zx}\rangle)/\sqrt{2}$, $|1^-\rangle = (|d_\downarrow^{yz}\rangle - i|d_\downarrow^{zx}\rangle)/\sqrt{2}$, $|2^+\rangle = (2|d_\uparrow^{xy}\rangle - |d_\downarrow^{yz}\rangle - i|d_\downarrow^{zx}\rangle)/\sqrt{6}$, $|2^-\rangle = (2|d_\downarrow^{xy}\rangle + |d_\uparrow^{yz}\rangle - i|d_\uparrow^{zx}\rangle)/\sqrt{6}$, respectively, where the quantization axis of spin is taken to be the z axis. Henceforth, we assume that the spin-orbit coupling in our system is sufficiently large and focus only on the case where the two multiplets, i.e., Γ_7 and Γ_8, do not hybridize with each other.

Now, we construct the normalized state $|g_j\rangle$ to minimize $\langle g_j| - U\vec{e}_j \cdot \vec{S}_j|g_j\rangle$ in the Hilbert space spanned by the states in Γ_7 or Γ_8. The desired states whose spins are parallel to the unit vector $\vec{e}_j$ are explicitly given for Γ_7 and Γ_8 by $|g_j^7\rangle = \sin(\theta_j/2)|3_j^+\rangle + e^{i\phi_j}\cos(\theta_j/2)|3_j^-\rangle$ and

$$|g_j^8\rangle = e^{-i(3/2)\phi_j}\cos^3(\theta_j/2)|1_j^+\rangle + e^{+i(3/2)\phi_j}\sin^3(\theta_j/2)|1_j^-\rangle - \sqrt{3}e^{-i(1/2)\phi_j}\sin(\theta_j/2)\cos^2(\theta_j/2)|2_j^+\rangle - \sqrt{3}e^{+i(1/2)\phi_j}\sin^2(\theta_j/2)\cos(\theta_j/2)|2_j^-\rangle, \quad (2)$$

respectively. Here subscript j denotes the site number and superscripts 7 and 8 correspond to Γ_7 and Γ_8, respectively. Using these states, we can derive the effective Hamiltonian $H = \sum_n T_n c_n^\dagger c_{n+1} + \text{H.c.} + V_n c_n^\dagger c_n$, where $c_n/c_n^\dagger$ denotes the renormalized annihilation or creation operator and the effective transfer integral T_n and site energy V_n are given as

$$T_n = \frac{2t}{3}\left(\sin\frac{\theta_n}{2}\sin\frac{\theta_{n+1}}{2} + e^{-i\Delta\phi}\cos\frac{\theta_n}{2}\cos\frac{\theta_{n+1}}{2}\right),$$

$V_n = -4t/3$, where $\Delta\phi = \phi_n - \phi_{n+1}$ for Γ_7, and

$$T_n = t\left(e^{i\Delta\phi/2}\cos\frac{\theta_n}{2}\cos\frac{\theta_{n+1}}{2} + e^{-i\Delta\phi/2}\sin\frac{\theta_n}{2}\sin\frac{\theta_{n+1}}{2}\right) \times \left(e^{i\Delta\phi}\cos^2\frac{\theta_n}{2}\cos^2\frac{\theta_{n+1}}{2} + e^{-i\Delta\phi}\sin^2\frac{\theta_n}{2}\sin^2\frac{\theta_{n+1}}{2}\right),$$

$V_n = -t(1 + \cos^2\theta_n)$ for Γ_8.

As for the Γ_7 case, we can write down T_n as $\frac{2t}{3}e^{ia_{n,n+1}}\cos\frac{\theta_{n,n+1}}{2}$, where $\theta_{n,n+1}$ is the angle between the two spins $\vec{S}_n$ and $\vec{S}_{n+1}$. The phase $a_{n,n+1}$ is the vector potential generated by the noncollinear spin configuration, but we can eliminate it by appropriate gauge transformation. Then we can conclude that we have no incommensurability in our 1D Γ_7 model.

As for the Γ_8 case, on the other hand, the effective site energy V_n explicitly depends on the local spin angle θ_n. If we have the spin configuration in the plane which is parallel to the xy plane, i.e., $\theta_n = \text{const}$, and set the pitch $\Delta\phi = \text{const}$, V_n and T_n are constant. On the other hand, if we have the tilt of the spin rotation plane from the above plane to the other plane, θ_n is no longer a constant and then V_n would generally be IC. $|T_n|$ also depends on both the angles of $\vec{S}_n$ and $\vec{S}_{n+1}$. Here we can conclude that in the case where holes are in Γ_8, the effective 1D model would generally be IC. This explains why the upper parts of the t_{2g} density of states in Fig. 1 are localized more strongly, where the wave function is mainly from Γ_8 components.

Now we focus on the Γ_8 case and numerically examine whether the localization of the wave function occurs in more details. We consider the helical spin configuration $\vec{S}_n = [S\cos(qn), S\cos\varphi\sin(qn), S\sin\varphi\sin(qn)]$, where q is the helical wave number, and φ denotes the tilt angle of the spin rotating plane from the xy plane (see Fig. 2).

The numerical calculations are performed for systems of size 1009, a large prime number, with nearly incommensurate modulations $q/2\pi = j/1009$, $(j = 1, 2, 3, \ldots)$. The results are shown in Figs. 3, where the vertical and the horizontal axes represent the energy and the helical wave number, respectively. We take the unit where $t = 1$ and $a = 1$. The tilt angles are $\varphi = 0°$, $30°$, $60°$, and $90°$ for Figs. 3(a)–3(d), respectively. The energy spectrum in Fig. 3(d) is almost same as the lowest band of Γ_8 bands in Fig. 1. In Fig. 3, the localization length increases as the color changes from blue to green. The figures clearly display that there are domains of strong localization $\xi \sim 1$ when we have a finite tilt angle φ. On the other hand, for $\varphi = 0°$ the transfer integrals T_n and the on-site potentials V_n are constants, and there are no localized states. Even in the most suitable case for localization, i.e., Fig. 3(d), however, the helical wave number q should be approximately in the range of $2\pi/3 < q < 4\pi/3$ for the localized states. This is because the long period of the helical structure means the slowly varying and weak perturbations in the rotated frame, and hence does not cause the localization.

Now we discuss the possible realization of the localized states in realistic systems. From the above results, three important conditions for the localization are (i) strong SOI, (ii) short helical period, and (iii) the direction of the rotating spin plane. The SOI increases as the mass of the atom gets heavier, and hence the present model becomes more relevant from the viewpoint (i). For $3d$ orbitals of transition metal oxides, the SOI is typically of the order of 20–30 meV, which is an order of magnitude smaller than the transfer integral t. Therefore the localization length is expected to be rather large, and hence the disorder effect such as the impurity scattering might hide the IC effect. Therefore, even though β-MnO_2 [11] and $SrFeO_3$ [12,13] show interesting transport properties, it is unlikely that the

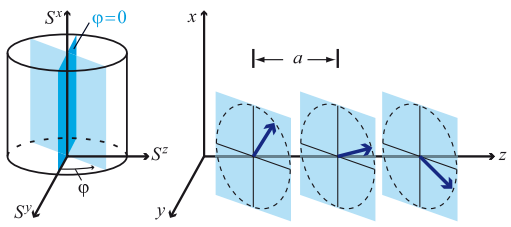

FIG. 2 (color online). Spin plane tilted by angle φ from the xy plane (left). The helical spins are rotating on the tilted plane placed periodically placed along the z axis. Blue arrows represent spins, while a denotes the lattice spacing (right).

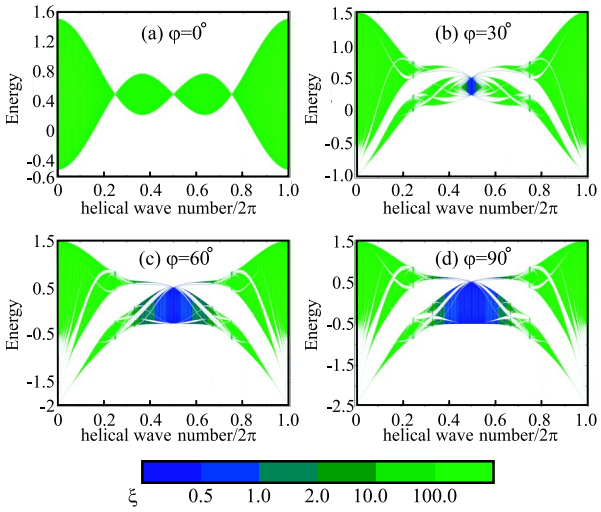

FIG. 3 (color online). Localization length ξ of the effective single-band model for the Γ_8 orbital with (a) $\varphi = 0°$, (b) $\varphi = 30°$, (c) $\varphi = 60°$, and (d) $\varphi = 90°$, respectively.

localization found in this Letter is relevant to these materials. $4d$ or $4f$, $5f$ orbitals, where SOI is larger than $\sim$0.3 eV, are more promising. Actually there are many rare-earth metals showing the helical spin structure such as Tb, Dy, Ho, Er [27,28]. From the condition (ii), it is rather hard to find the short period helical spin structure. It is typically $4a$-$5a$ or even larger [12,14,27,28]. From this viewpoint, MnO_2 [1,11] is an interesting case, but the localization is unlikely as discussed above. As for the condition (iii), we need more study since only the cubic case has been considered. The directional dependence of the spin plane might be useful to control the L-DL by an external magnetic field.

Even though the conditions for localization discussed above are rather stringent, which explains why it has never been observed experimentally thus far, it will play a vital role in the quantum transport properties of the system once realized. One direct consequence is the large anisotropy of the resistivity between parallel and perpendicular to the helical axis, i.e., it should be much more resistive in the parallel direction [29]. This can be detected, for example, as a drastic change of the resistivity anisotropy at the commensurate-incommensurate transition.

In conclusion, we have studied the localization or delocalization of the electronic states in helical magnets. We found the localized states under the condition of (i) strong spin-orbit interaction, (ii) short helical wavelength, and (iii) proper direction of the plane on which spins rotate. The strong dependence of the localization length ξ on the orbital is also found, which is explained by an effective model for a certain limiting case.

The authors are grateful to S. Miyashita, Y. Shimada, and K. Azuma for fruitful discussions. This work was supported by NAREGI Grant, the Ministry of Education, Culture, Sports, Science and Technology of Japan, Grant-in-Aids for Scientific Research (S), 15104006, 2003; 17105002, 2005; and Scientific Research on Priority Areas, 16076205, 2004.

*Electronic address: shu-t@spin.phys.s.u-tokyo.ac.jp

[1] A. Yoshimori, J. Phys. Soc. Jpn. **14**, 807 (1959).
[2] T. Nagamiya, in *Solid State Physics*, edited by F. Seitz, D. Turnbull, and H. Ehrenreich (Academic, New York, 1967), Vol. 20, p. 305.
[3] H. Katsura, N. Nagaosa, and A. V. Balatsky, Phys. Rev. Lett. **95**, 057205 (2005).
[4] T. Kimura *et al.*, Nature (London) **426**, 55 (2003).
[5] T. Goto *et al.*, Phys. Rev. Lett. **92**, 257201 (2004).
[6] M. Kenzelmann *et al.*, Phys. Rev. Lett. **95**, 087206 (2005).
[7] T. Kimura, G. Lawes, and A. P. Ramirez, Phys. Rev. Lett. **94**, 137201 (2005).
[8] G. Lawes *et al.*, Phys. Rev. Lett. **95**, 087205 (2005).
[9] L. C. Chapon *et al.*, Phys. Rev. Lett. **93**, 177402 (2004).
[10] G. R. Blake *et al.*, Phys. Rev. B **71**, 214402 (2005).
[11] H. Sato *et al.*, Phys. Rev. B **61**, 3563 (2000).
[12] T. Takeda, Y. Yamaguchi, and H. Watanabe, J. Phys. Soc. Jpn. **33**, 967 (1972).
[13] M. Takano (private communications).
[14] N. Manyala *et al.*, Nature (London) **408**, 616 (2000).
[15] P. W. Anderson and H. Hasegawa, Phys. Rev. **100**, 675 (1955).
[16] X. G. Wen, F. Wilczek, and A. Zee, Phys. Rev. B **39**, 11 413 (1989).
[17] N. Nagaosa and P. A. Lee, Phys. Rev. Lett. **64**, 2450 (1990).
[18] J. B. Sokoloff, Phys. Rep. **126**, 189 (1985).
[19] S. Aubry and G. Andre, Ann. Isr. Phys. Soc. **3**, 133 (1979).
[20] D. R. Hofstadter, Phys. Rev. B **14**, 2239 (1976).
[21] M. Kohmoto, L. P. Kadanoff, and C. Tang, Phys. Rev. Lett. **50**, 1870 (1983).
[22] M. Kohmoto, B. Sutherland, and C. Tang, Phys. Rev. B **35**, 1020 (1987).
[23] S. Sugano, Y. Tanabe, and H. Kamimura, *Multiplets of Transition-Metal Ions in Crystals* (Academic, New York, 1970).
[24] W. A. Harrison, *Elementary Electronic Structure* (World Scientific, Singapore, 1999), p. 546.
[25] A. MacKinnon and B. Kramer, Z. Phys. B **53**, 1 (1983), and references therein.
[26] An early work [C. M. Soukoulis and E. N. Economou, Phys. Rev. Lett. **48**, 1043 (1982)] also found the mobility edge in a model with the generalized potential $\epsilon_n = V_0[\cos(Qn) + V_1 \cos(2Qn)]$ (Q : IC wave number) similarly to our case.
[27] W. C. Koehler, J. Appl. Phys. **36**, 1078 (1965).
[28] R. A. Cowley *et al.*, Phys. Rev. B **57**, 8394 (1998).
[29] A recent study (M. Onoda and N. Nagaosa, cond-mat/0604120) has shown that the disorder turns the localized states along the parallel direction to IC wave vector into an anisotropic metallic state.